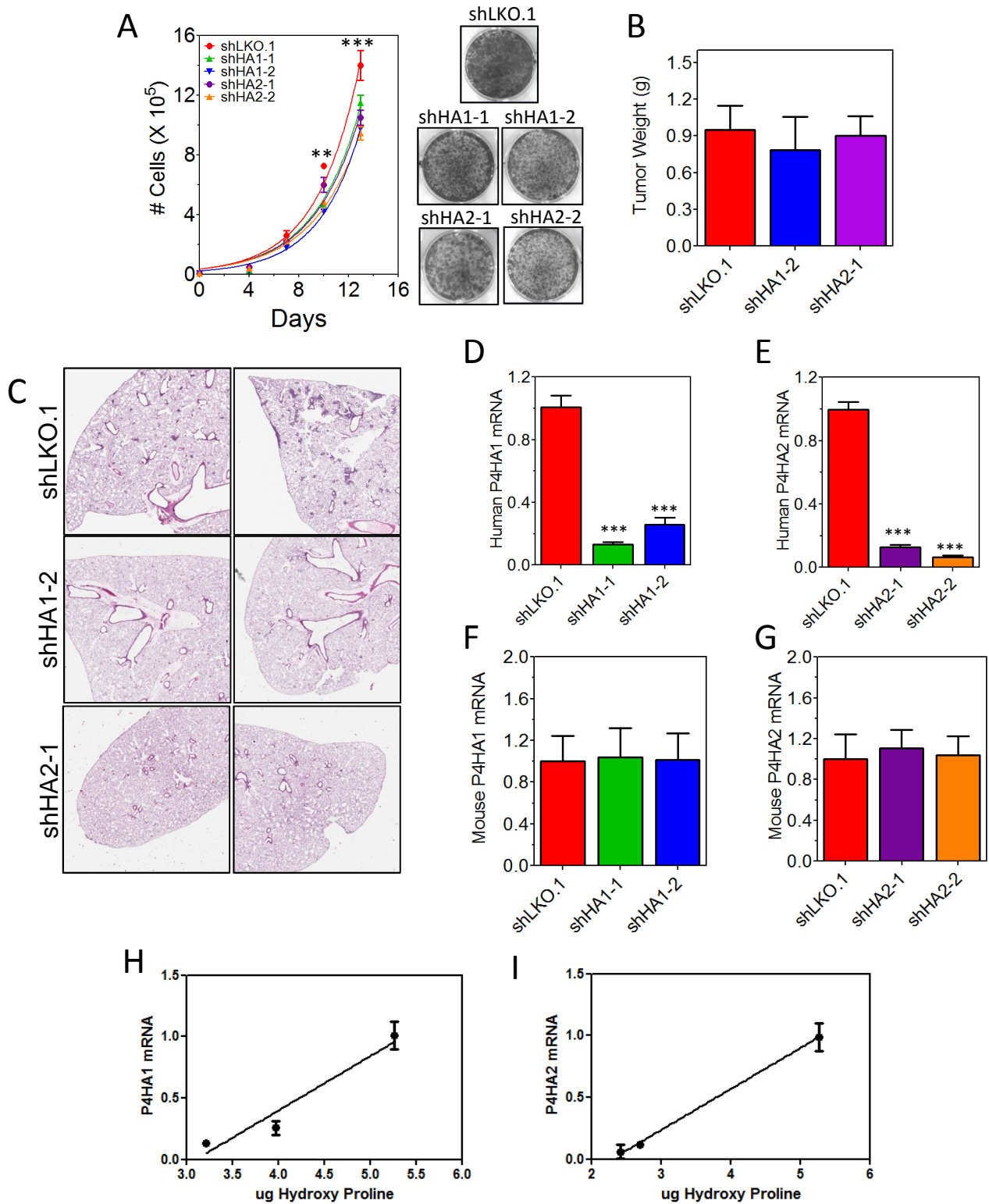


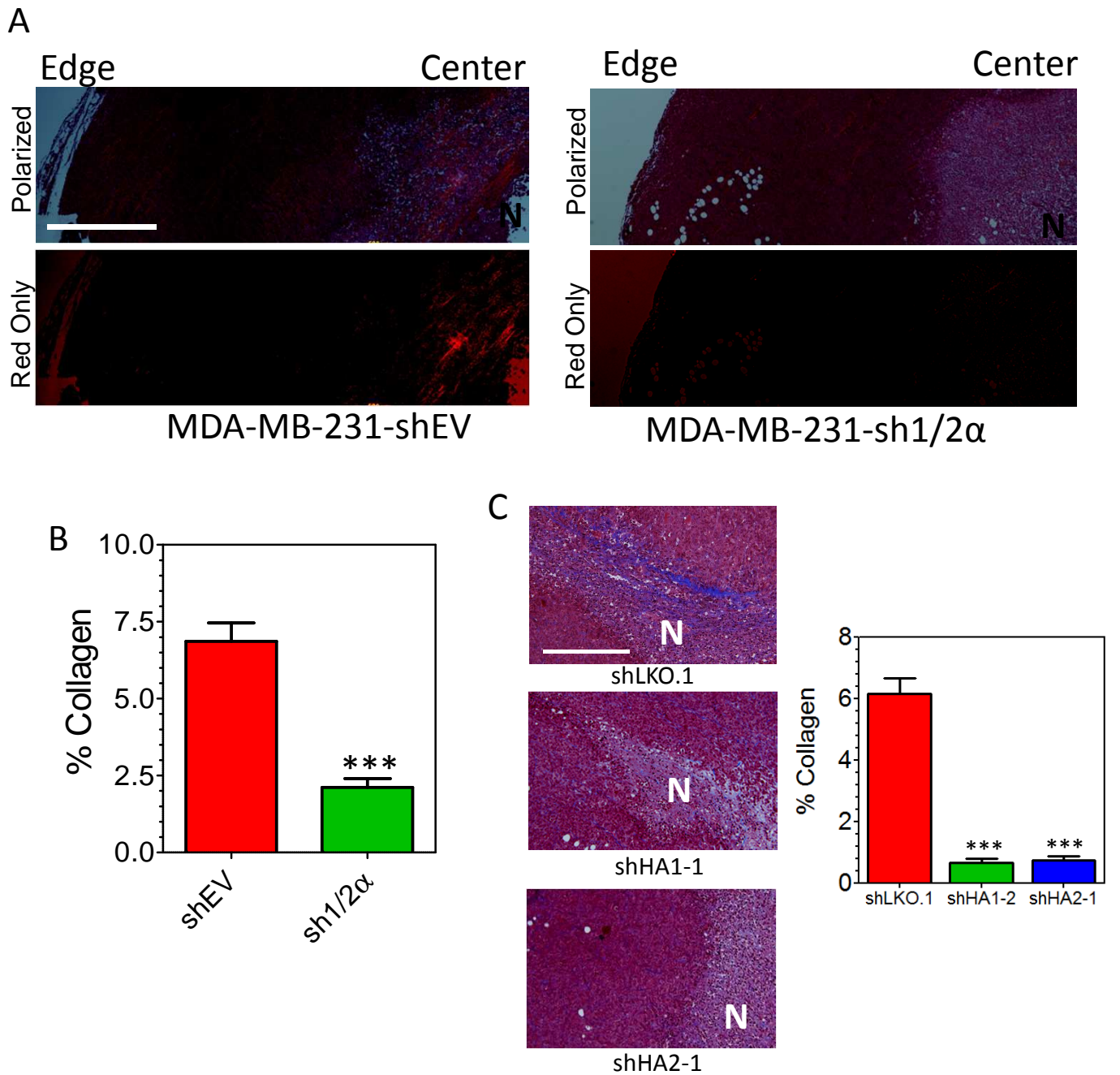
Supplementary Figure S1, HIF-1 dependent P4HA1 and P4HA2 induction

A, MDA-MB-231 cells were treated with 200 nM digoxin or vehicle control (0.02% DMSO) during exposure to 20% or 1% O₂ for 24 hours. P4HA1 and P4HA2 mRNA levels were assessed by RT-qPCR (mean ± SEM, *n* = 3, one-way ANOVA). B, HIF1α, P4HA1, and P4HA2 protein levels were assessed by immunoblot assays of MDA-MB-231 cells following 0, 12, 24, 48, and 72 hours of exposure to 1% O₂. C, HIF1α, P4HA1, and P4HA2 protein levels were assessed by immunoblot assays of lysates prepared from MDA-MB-231, MCF-7, and MCF10A cells exposed to 20% or 1% O₂ for 48 hours. D, Immunoblot assays were performed on tissue lysates from orthotopically-derived MDA-MB-231-shEV and MDA-MB-231-sh1/2α primary breast tumors. E, Images from Figure 1D (shEV) were deconvoluted and pseudocolored to assess colocalization. Scale bar = 150 μm.



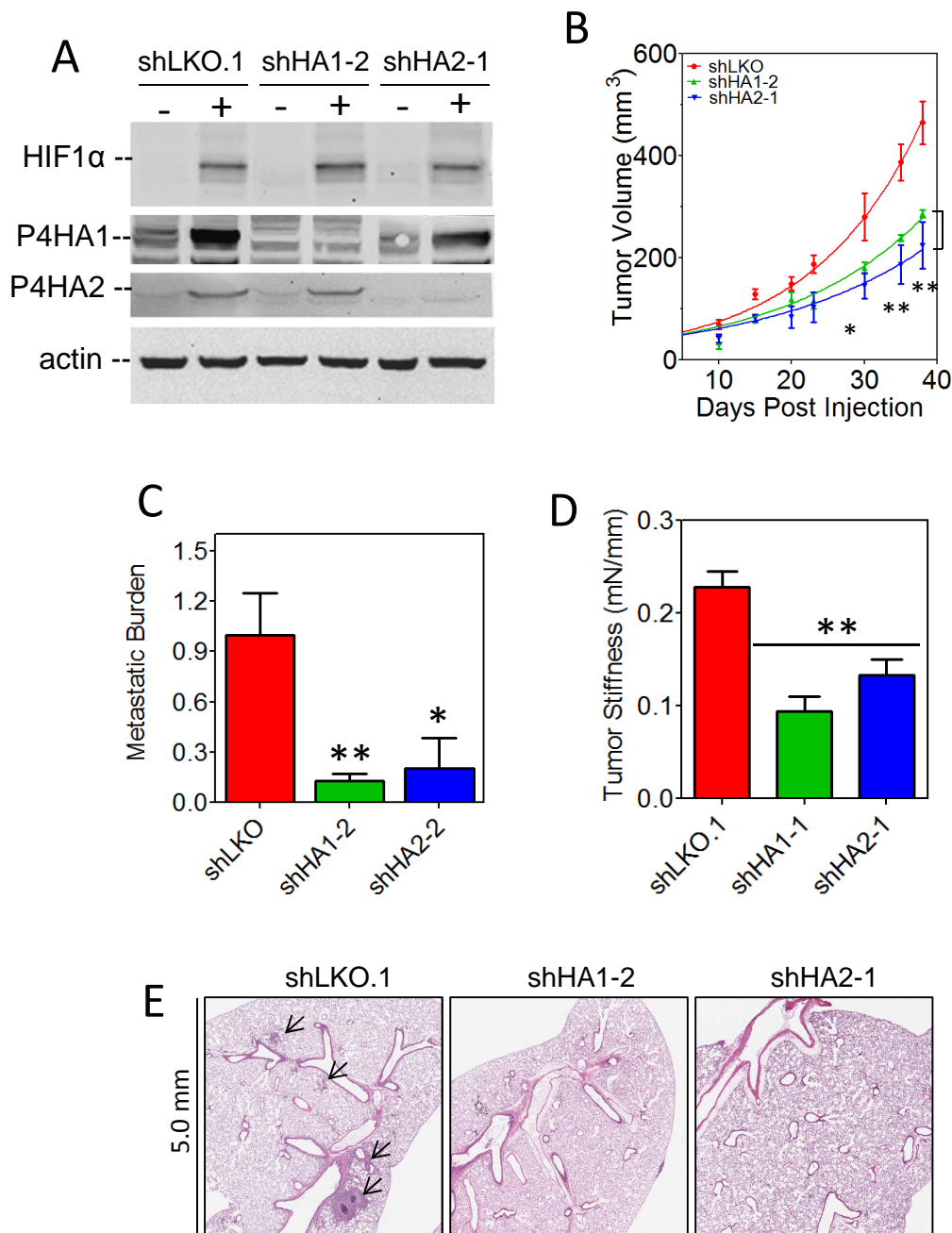
Supplementary Figure S2, P4HA1 and P4HA2 knockdown inhibits breast cancer growth and metastasis

A, proliferation of cultured MDA-MB-231 subclones was determined by trypan blue staining followed by cell counting on days indicated. Growth curves of control (shLKO.1) and P4HA1 (shHA1-1 and shHA1-2) and P4HA2 (shHA2-1 and shHA2-2) knockdown cells are plotted (mean \pm SD, $n=3$, two-way ANOVA). Crystal violet staining following 10 days of culture is shown (right). B, final weight (in grams) of tumors analyzed in Figure 2F is plotted (mean \pm SEM, $n = 5$, one-way ANOVA). C, representative H&E staining of lung sections from 2 mice per group is shown. D-G, human P4HA1 (D), human P4HA2 (E), mouse P4HA1 (F), and mouse P4HA2 (G) mRNA expression in MFP tumors were determined by RT-qPCR (mean \pm SEM, $n = 5$, one-way ANOVA with Bonferroni post-test). *** $P < 0.001$ vs. shLKO.1. H-I, The relative P4HA1 (H) or P4HA2 (I) mRNA levels from tumor lysate was compared to the hydroxyproline content from the same tumor lysate.



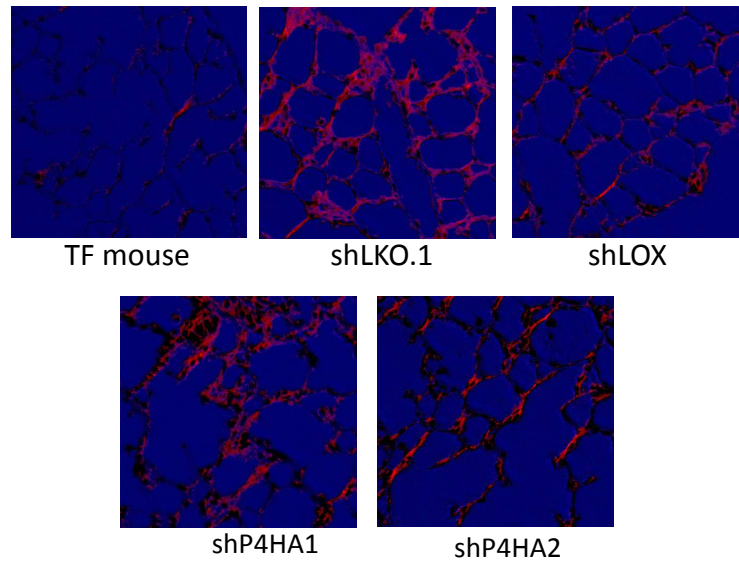
Supplementary Figure S3, Collagen hydroxylase knockdown decreases collagen deposition *in vivo*

A, tumor sections from MDA-MB-231-shEV and MDA-MB-231-sh1/2 α cells were stained with picosirius red and imaged under circularly polarized light. Scale bar = 1 mm. B, the area of red staining (bottom row, A) divided by the total area of the tumor section was determined using image analysis for 5 mice per group and 3 sections per mouse (mean \pm SEM, $n = 15$, one-way ANOVA with Bonferroni post-test). ** $P < 0.01$ vs. shEV. C, Masson trichrome staining of MDA-MB-231-shLKO.1 and shHA1-1 or shHA2-1 tumor sections. Collagen fibers are stained in blue. Graph shows the % percent area of blue staining compared to the total area of the section. N, necrosis. Scale bar = 250 μ m.



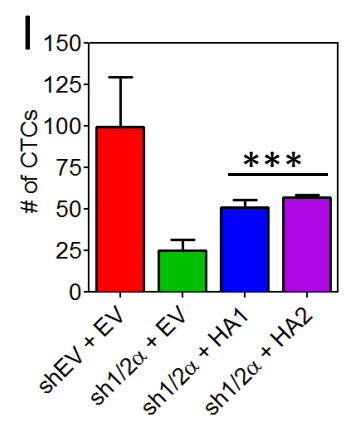
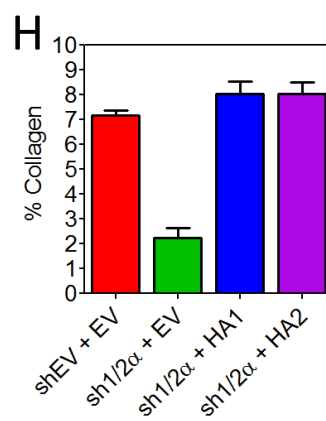
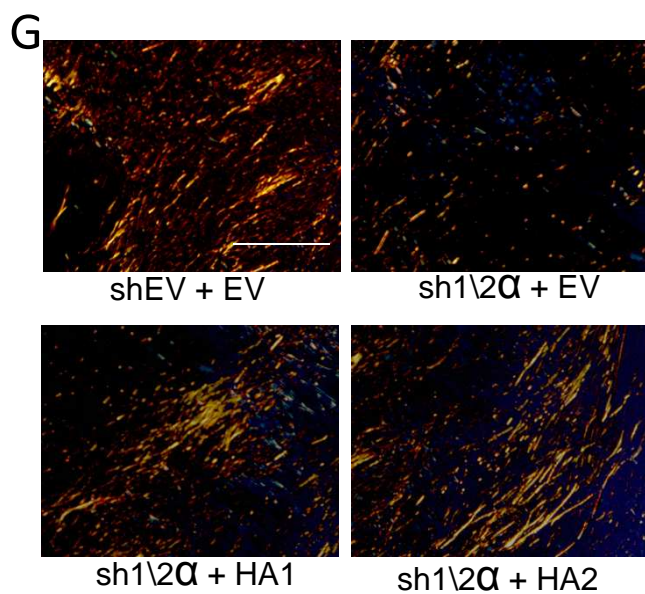
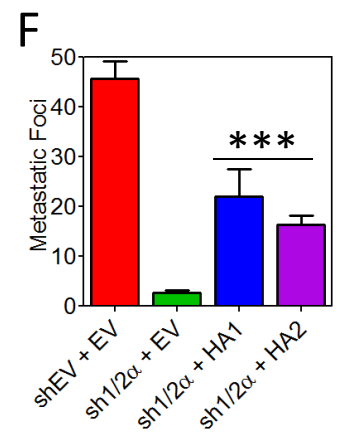
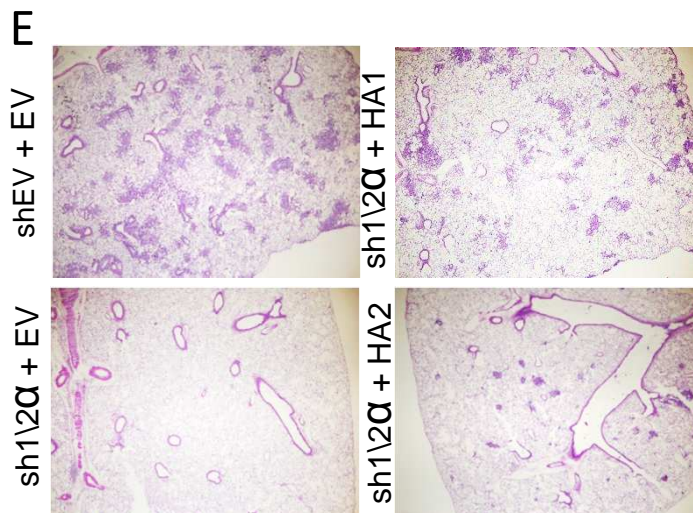
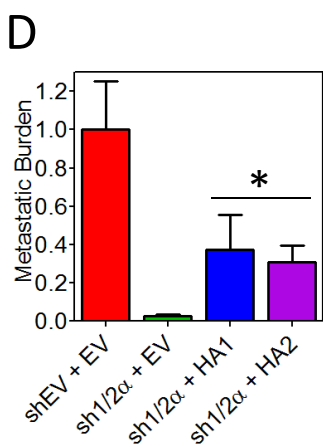
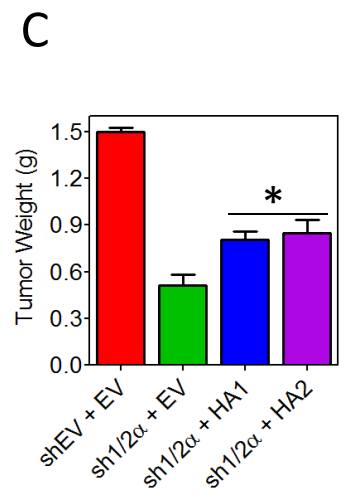
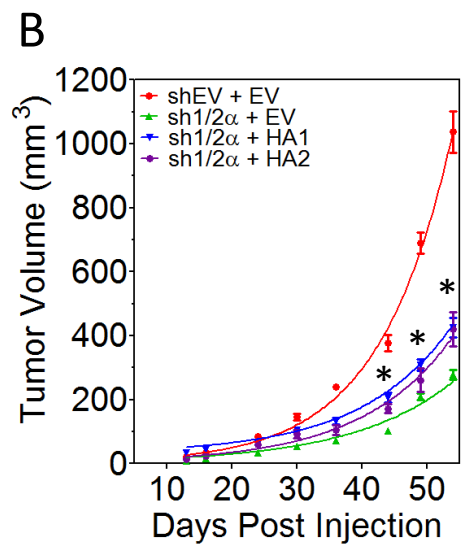
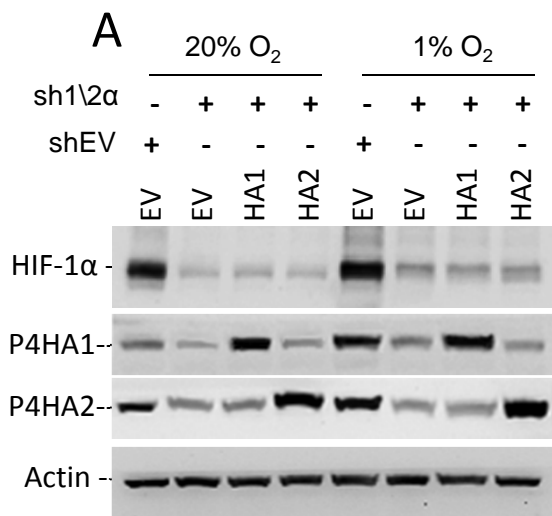
Supplementary Figure S4, P4HA1 and P4HA2 knockdown inhibits growth and metastasis of MDA-MB-435 cells

A, HIF1 α , P4HA1 and P4HA2 protein levels were determined by immunoblot assay of lysates prepared from MDA-MB-435 shLKO.1, shHA1-2, and shHA2-1 knockdown cells exposed to 20% or 1% O₂ for 48 hours. B, tumors were derived from the orthotopic injection of MDA-MB-435 control and knockdown cells described into the MFP of NOD-SCID mice ($n = 5$ mice per group) and tumor volume was plotted versus time (Mean \pm SEM ($n = 5$), two-way ANOVA). C, human genomic DNA content in mouse lungs was quantified using qPCR with human specific *HK2* primers (one-way ANOVA). D, the stiffness of freshly dissected MDA-MB-435 tumors was determined using an indentation device for 5 tumors with 5 points per tumor (mean \pm SEM ($n = 25$), one-way ANOVA). E, representative H&E sections are shown. Bonferroni post-test was conducted for all ANOVA experiments * $P < 0.05$, ** $P < 0.01$ vs. shLKO.1.



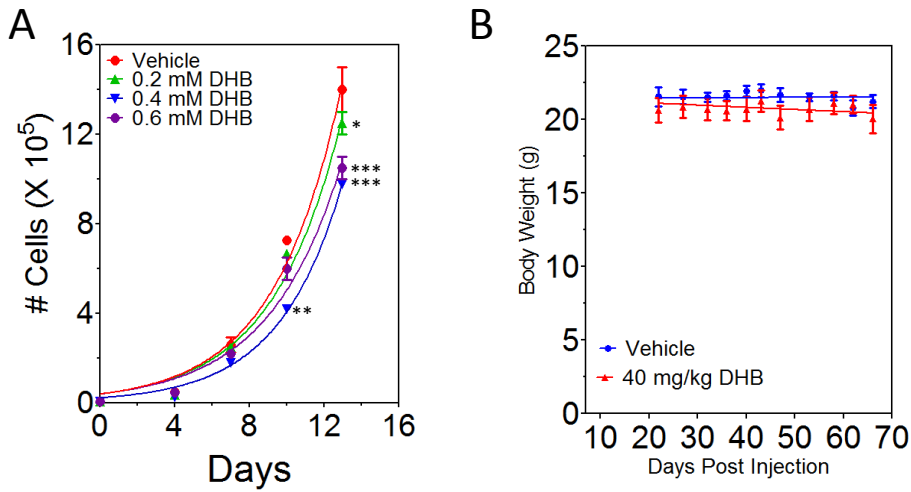
Supplementary Figure S5, Picosirius red staining of mouse lungs

Lung sections from mice which were tumor-free (TF) or injected with the indicated MDA-MB-231 subclones were stained with picosirius red and imaged under circularly polarized light.



Supplementary Figure S6, P4HA re-expression in HIF-deficient cells rescues collagen deposition and metastasis

Collagen prolyl hydroxylase overexpression increases metastasis of MDA-MB-231 shHIF-1/2 α cells. A, immunoblot assays were performed to determine P4HA1 and P4HA2 protein levels in MDA-MB-231 control (shEV) or shHIF-1 α and shHIF-2 α double knockdown cells (sh1/2 α) stably expressing either a control (EV), P4HA1 (HA1) or P4HA2 (HA2) lentiviral expression vector following exposure to 20% or 1% O₂ for 48 hours. B, MDA-MB-231 subclones were injected into the MFP of NOD-SCID mice. Tumor volume was plotted versus time (mean \pm SEM, $n = 5$, two-way ANOVA). C, final tumor weight (in grams; mean \pm SEM, $n = 5$) was determined. D, human DNA content in mouse lungs was determined by qPCR (mean \pm SEM, $n = 5$, one-way ANOVA). E, lung sections were stained with hematoxylin and eosin (3 X 3 mm section). F, the number of metastases per field was determined (mean \pm SEM, $n = 10$, one-way). G, tumor sections were stained with picosirius red and imaged under circularly polarized light. Scale bar = 400 μ m. H, the area of red staining relative to total area of the tumor section was determined using image analysis. I, peripheral blood (0.5 mL) was collected from each mouse. Human 18S rRNA expression was quantified using qPCR and the number of circulating tumor cells (CTCs) was determined. (mean \pm SEM, $n = 5$, one-way ANOVA). Bonferroni post-test was performed for all ANOVAs. * $P < 0.05$, ** $P < 0.01$, *** $P < 0.001$ vs. sh1/2 α + EV.



Supplementary Figure S7, DHB treatment of MDA-MB-231 Cells

A, MDA-231 Cells were treated with the indicated doses of DHB. Cell proliferation in tissue culture was determined by trypan blue staining followed by cell counting on the indicated days (mean \pm SEM, $n = 3$, two-way ANOVA with Bonferroni post-test) * $P < 0.05$, ** $P < 0.01$, *** $P < 0.001$ vs. vehicle-treated MDA-MB-231 cells. B, body weight of DHB- or vehicle-treated mice were measured on the indicated days.

Primer	Sequence
P4HA1 FW (human)	CCCTGAGACTGGAAAATTGACCACAGC
P4HA1 REV (human)	GGGGTTCATACTGTCCTCCA ACTCCA
P4HA1 FW (mouse)	ACACTGAGTGGAGTGAGTTGG
P4HA1 Rev (mouse)	TTGCAGCCGAAACAGAGCTT
P4HA1 FW (human and mouse)	GCTGTGGATTACCTGCCAGAGAGA
P4HA1 Rev (human and mouse)	TACCCTCCCCACGGCACAGC
P4HA2 FW (human)	GCCTGCGCTGGAGGACCTTG
P4HA2 REV (human)	TGTGCCTGGGTCCAGCCTGT
P4HA2 FW (mouse)	TTGCTAAGCCCAA ACTTGAC
P4HA2 Rev (mouse)	GCATCTTCGTCATCGCTCCT
P4HA2 FW (human and mouse)	CTCACCCGCCGCCTGCTCTC
P4HA2 REV (human and mouse)	CCCTCCAGCTCGTTCGTGGC
HK2 FW (human)	CCAGTTCATTCACATCATCAG
HK2 REV (human)	CTTACACGAGGTCACATAGC

Supplementary Table S1, Real-Time qPCR primers.

FW, forward primer; REV, reverse primer.

Human P4HA1 / Total P4HA1 mRNA	Mouse P4HA1 / Total P4HA1 mRNA
0.89	0.07
0.92	0.07
0.87	0.09
0.86	0.05
0.74	0.20
0.88	0.10
0.89	0.07
<i>Mean = 0.86 (± .057)</i>	<i>Mean = 0.09 (± .05)</i>

Supplemental Table S2, Comparison of human P4HA1 mRNA versus mouse P4HA1 mRNA expression in tumors

Comparison of human P4HA1 mRNA versus mouse P4HA1 mRNA expression in MDA-MB-231-shLKO.1 tumors. Three independent P4HA1 primer pairs were utilized for RT-qPCR analysis: a human-specific P4HA1 primer, a mouse-specific P4HA1 primer, a primer that recognized both mouse and human P4HA1 (total). Bottom row: mean + /- standard deviation.

P4HA1 mRNA		P4HA2 mRNA	
Status	p-value	Status	p-value
ER+ v. ER-	0.22	ER+ v. ER-	0.33
PR+ v. PR-	0.88	PR+ v. PR-	0.53
HER2+ v. HER2-	<0.05	HER2+ v. HER2-	<0.005
DN v. All	0.21	DN v. All	0.18
TN v. All	0.41	TN v. All	0.20

Supplemental Table S3, Correlation of P4HA1 and P4HA2 mRNA expression with receptor status

Correlation (p-value) of human P4HA1 or P4HA2 mRNA expression in cancer genome atlas patient samples (Figure 6C) based on estrogen receptor (ER), progesterone receptor (PR), HER2 receptor, double negative (ER-/PR-) DN, or triple negative (ER-/PR-/HER2-) TN patient status used to group data for comparison.